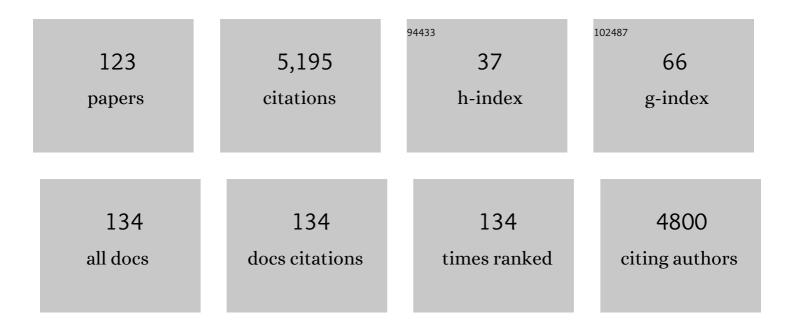
Martin O Saar

List of Publications by Year in descending order

Source: https://exaly.com/author-pdf/4726913/publications.pdf Version: 2024-02-01



Μαρτινι Ο ςλαρ

#	Article	IF	CITATIONS
1	Numerical analysis and optimization of the performance of CO2-Plume Geothermal (CPG) production wells and implications for electric power generation. Geothermics, 2022, 98, 102270.	3.4	26
2	Flexible CO2-plume geothermal (CPG-F): Using geologically stored CO2 to provide dispatchable power and energy storage. Energy Conversion and Management, 2022, 253, 115082.	9.2	15
3	Accelerated reactive transport simulations in heterogeneous porous media using Reaktoro and Firedrake. Computational Geosciences, 2022, 26, 295-327.	2.4	4
4	Techno-economic analysis of Advanced Geothermal Systems (AGS). Renewable Energy, 2022, 186, 927-943.	8.9	7
5	Multi-disciplinary characterizations of the BedrettoLab – a new underground geoscience research facility. Solid Earth, 2022, 13, 301-322.	2.8	17
6	On the applicability of connectivity metrics to rough fractures under normal stress. Advances in Water Resources, 2022, 161, 104122.	3.8	5
7	On the validation of mixed-mode I/II crack growth theories for anisotropic rocks. International Journal of Solids and Structures, 2022, 241, 111484.	2.7	18
8	Numerical Modeling of the Effects of Pore Characteristics on the Electric Breakdown of Rock for Plasma Pulse Geo Drilling. Energies, 2022, 15, 250.	3.1	4
9	On Reliable Prediction of Fracture Path in Anisotropic Rocks. Procedia Structural Integrity, 2022, 39, 792-800.	0.8	1
10	Modelling Potential Geological CO2 Storage Combined with CO2-Plume Geothermal CPG Energy Extraction in Switzerland. , 2022, , .		0
11	Review: Induced Seismicity During Geoenergy Development—A Hydromechanical Perspective. Journal of Geophysical Research: Solid Earth, 2022, 127, .	3.4	21
12	Shear induced fluid flow path evolution in rough-wall fractures: A particle image velocimetry examination. Journal of Hydrology, 2022, 610, 127793.	5.4	3
13	The Importance of Modeling Carbon Dioxide Transportation and Geologic Storage in Energy System Planning Tools. Frontiers in Energy Research, 2022, 10, .	2.3	7
14	Using <mml:math <br="" xmlns:mml="http://www.w3.org/1998/Math/MathML">altimg="si1.svg"><mml:msub><mml:mtext>CO</mml:mtext><mml:mn>2</mml:mn></mml:msub></mml:math> - geothermal (CPG) energy technologies to support wind and solar power in renewable-heavy electricity systems. Renewable and Sustainable Energy Transition, 2022, 2, 100026.	Plume 2.9	2
15	Relating Darcy-Scale Chemical Reaction Order to Pore-Scale Spatial Heterogeneity. Transport in Porous Media, 2022, 144, 507-543.	2.6	1
16	The value of CO2-Bulk energy storage with wind in transmission-constrained electric power systems. Energy Conversion and Management, 2021, 228, 113548.	9.2	9
17	Quantification of mineral accessible surface area and flow-dependent fluid-mineral reactivity at the pore scale. Chemical Geology, 2021, 563, 120042.	3.3	15
18	Noâ€Flow Fraction (NFF) Permeability Model for Rough Fractures Under Normal Stress. Water Resources Research, 2021, 57, e2020WR029080.	4.2	18

#	Article	IF	CITATIONS
19	Integrated magnetotelluric and petrological analysis of felsic magma reservoirs: Insights from Ethiopian rift volcanoes. Earth and Planetary Science Letters, 2021, 559, 116765.	4.4	19
20	Minimum transmissivity and optimal well spacing and flow rate for high-temperature aquifer thermal energy storage. Applied Energy, 2021, 289, 116658.	10.1	15
21	Heat depletion in sedimentary basins and its effect on the design and electric power output of CO2 Plume Geothermal (CPG) systems. Renewable Energy, 2021, 172, 1393-1403.	8.9	30
22	Flow-through Drying during CO2 Injection into Brine-filled Natural Fractures: A Tale of Effective Normal Stress. International Journal of Greenhouse Gas Control, 2021, 109, 103378.	4.6	1
23	Simulating Plasma Formation in Pores under Short Electric Pulses for Plasma Pulse Geo Drilling (PPGD). Energies, 2021, 14, 4717.	3.1	10
24	Sensitivity of Reservoir and Operational Parameters on the Energy Extraction Performance of Combined CO2-EGR–CPG Systems. Energies, 2021, 14, 6122.	3.1	9
25	Benchmark study of simulators for thermo-hydraulic modelling of low enthalpy geothermal processes. Geothermics, 2021, 96, 102130.	3.4	5
26	A lattice-Boltzmann study of permeability-porosity relationships and mineral precipitation patterns in fractured porous media. Computational Geosciences, 2020, 24, 1865-1882.	2.4	14
27	Hydraulic stimulation and fluid circulation experiments in underground laboratories: Stepping up the scale towards engineered geothermal systems. Geomechanics for Energy and the Environment, 2020, 24, 100175.	2.5	55
28	A combined thermo-mechanical drilling technology for deep geothermal and hard rock reservoirs. Geothermics, 2020, 85, 101771.	3.4	32
29	Combining brine or CO2 geothermal preheating with low-temperature waste heat: A higher-efficiency hybrid geothermal power system. Journal of CO2 Utilization, 2020, 42, 101323.	6.8	14
30	Synchrotron-based pore-network modeling of two-phase flow in Nubian Sandstone and implications for capillary trapping of carbon dioxide. International Journal of Greenhouse Gas Control, 2020, 103, 103164.	4.6	15
31	Field test of a Combined Thermo-Mechanical Drilling technology. Mode I: Thermal spallation drilling. Journal of Petroleum Science and Engineering, 2020, 190, 107005.	4.2	15
32	Permeability Impairment and Salt Precipitation Patterns During CO ₂ Injection Into Single Natural Brineâ€Filled Fractures. Water Resources Research, 2020, 56, e2020WR027213.	4.2	14
33	Increased Power Generation due to Exothermic Water Exsolution in CO2 Plume Geothermal (CPG) Power Plants. Geothermics, 2020, 88, 101865.	3.4	28
34	Coulomb criterion - bounding crustal stress limit and intact rock failure: Perspectives. Powder Technology, 2020, 374, 106-110.	4.2	8
35	Contact between rough rock surfaces using a dual mortar method. International Journal of Rock Mechanics and Minings Sciences, 2020, 133, 104414.	5.8	4
36	Combining natural gas recovery and CO2-based geothermal energy extraction for electric power generation. Applied Energy, 2020, 269, 115012.	10.1	70

#	Article	IF	CITATIONS
37	The Effect of Mineral Dissolution on the Effective Stress Law for Permeability in a Tight Sandstone. Geophysical Research Letters, 2020, 47, e2020GL088346.	4.0	10
38	A numerical investigation into key factors controlling hard rock excavation via electropulse stimulation. Journal of Rock Mechanics and Geotechnical Engineering, 2020, 12, 793-801.	8.1	22
39	ModeÂl fracture growth in anisotropic rocks: Theory and experiment. International Journal of Solids and Structures, 2020, 195, 74-90.	2.7	65
40	Corrigendum to "Hydraulic stimulation and fluid circulation experiments in underground laboratories: Stepping up the scale towards engineered geothermal systems―by Gischig et al. https://doi.org/10.1016/j.gete.2019.100175. Geomechanics for Energy and the Environment, 2020, 24, 100190.	2.5	2
41	Simulation of rock failure modes in thermal spallation drilling. Acta Geotechnica, 2020, 15, 2327-2340.	5.7	16
42	On the directional dependency of Mode I fracture toughness in anisotropic rocks. Theoretical and Applied Fracture Mechanics, 2020, 107, 102494.	4.7	35
43	Field test of a Combined Thermo-Mechanical Drilling technology. Mode II: Flame-assisted rotary drilling. Journal of Petroleum Science and Engineering, 2020, 190, 106880.	4.2	15
44	Modelling of hydro-mechanical processes in heterogeneous fracture intersections using a fictitious domain method with variational transfer operators. Computational Geosciences, 2020, 24, 1799-1814.	2.4	6
45	Accelerating Reactive Transport Modeling: On-Demand Machine Learning Algorithm for Chemical Equilibrium Calculations. Transport in Porous Media, 2020, 133, 161-204.	2.6	23
46	The influence of thermal treatment on rock–bit interaction: a study of a combined thermo–mechanical drilling (CTMD) concept. Geothermal Energy, 2020, 8, .	1.9	10
47	Solute tracer test quantification of the effects of hot water injection into hydraulically stimulated crystalline rock. Geothermal Energy, 2020, 8, .	1.9	11
48	3D non-conforming mesh model for flow in fractured porous media using Lagrange multipliers. Computers and Geosciences, 2019, 132, 42-55.	4.2	32
49	Field Comparison of DNA‣abeled Nanoparticle and Solute Tracer Transport in a Fractured Crystalline Rock. Water Resources Research, 2019, 55, 6577-6595.	4.2	35
50	Thermally driven fracture aperture variation in naturally fractured granites. Geothermal Energy, 2019, 7, .	1.9	23
51	Using TNT-NN to unlock the fast full spatial inversion of large magnetic microscopy data sets. Earth, Planets and Space, 2019, 71, .	2.5	5
52	Simulation of hydro-mechanically coupled processes in rough rock fractures using an immersed boundary method and variational transfer operators. Computational Geosciences, 2019, 23, 1125-1140.	2.4	10
53	A methodology to determine the elastic properties of anisotropic rocks from a single uniaxial compression test. Journal of Rock Mechanics and Geotechnical Engineering, 2019, 11, 1166-1183.	8.1	42
54	Toward a Spatiotemporal Understanding of Dolomite Dissolution in Sandstone by CO ₂ -Enriched Brine Circulation. Environmental Science & Technology, 2019, 53, 12458-12466.	10.0	14

#	Article	IF	CITATIONS
55	On the direct measurement of shear moduli in transversely isotropic rocks using the uniaxial compression test. International Journal of Rock Mechanics and Minings Sciences, 2019, 113, 220-240.	5.8	32
56	The value of bulk energy storage for reducing CO2 emissions and water requirements from regional electricity systems. Energy Conversion and Management, 2019, 181, 674-685.	9.2	24
57	Modified semi-circular bend test to determine the fracture toughness of anisotropic rocks. Engineering Fracture Mechanics, 2019, 213, 153-171.	4.3	50
58	High-Resolution Temporo-Ensemble PIV to Resolve Pore-Scale Flow in 3D-Printed Fractured Porous Media. Transport in Porous Media, 2019, 129, 467-483.	2.6	21
59	Demonstration of thermal borehole enlargement to facilitate controlled reservoir engineering for deep geothermal, oil or gas systems. Applied Energy, 2018, 212, 1501-1509.	10.1	26
60	Magnetotelluric Image of Transcrustal Magmatic System Beneath the Tulu Moye Geothermal Prospect in the Ethiopian Rift. Geophysical Research Letters, 2018, 45, 12,847.	4.0	58
61	Silica-Encapsulated DNA-Based Tracers for Aquifer Characterization. Environmental Science & Technology, 2018, 52, 12142-12152.	10.0	50
62	Estimating fluid flow rates through fracture networks using combinatorial optimization. Advances in Water Resources, 2018, 122, 85-97.	3.8	10
63	Tomographic Reservoir Imaging with DNA-Labeled Silica Nanotracers: The First Field Validation. Environmental Science & Technology, 2018, 52, 13681-13689.	10.0	35
64	The seismo-hydromechanical behavior during deep geothermal reservoir stimulations: open questions tackled in a decameter-scale in situ stimulation experiment. Solid Earth, 2018, 9, 115-137.	2.8	126
65	TNT: A Solver for Large Dense Least-Squares Problems that Takes Conjugate Gradient from Bad in Theory, to Good in Practice. , 2018, , .		1
66	The Effects of High Heating Rate and High Temperature on the Rock Strength: Feasibility Study of a Thermally Assisted Drilling Method. Rock Mechanics and Rock Engineering, 2018, 51, 2957-2964.	5.4	88
67	Permeability, porosity, and mineral surface area changes in basalt cores induced by reactive transport of <scp>CO</scp> ₂ â€rich brine. Water Resources Research, 2017, 53, 1908-1927.	4.2	65
68	Whole rock basalt alteration from CO2-rich brine during flow-through experiments at 150 ŰC and 150 bar. Chemical Geology, 2017, 453, 92-110.	3.3	52
69	An overview of computational methods for chemical equilibrium and kinetic calculations for geochemical and reactive transport modeling. Pure and Applied Chemistry, 2017, 89, 597-643.	1.9	45
70	A Hybrid Geothermal Energy Conversion Technology - A Potential Solution for Production of Electricity from Shallow Geothermal Resources. Energy Procedia, 2017, 114, 7107-7117.	1.8	17
71	TNT-NN: A Fast Active Set Method for Solving Large Non-Negative Least Squares Problems. Procedia Computer Science, 2017, 108, 755-764.	2.0	15
72	Calculating thermophysical fluid properties during geothermal energy production with NESS and Reaktoro. Geothermics, 2017, 70, 146-154.	3.4	13

#	Article	IF	CITATIONS
73	Multifluid geo-energy systems: Using geologic CO ₂ storage for geothermal energy production and grid-scale energy storage in sedimentary basins. , 2016, 12, 678-696.		41
74	Computational methods for reactive transport modeling: An extended law of mass-action, xLMA, method for multiphase equilibrium calculations. Advances in Water Resources, 2016, 96, 405-422.	3.8	16
75	Enabling Gibbs energy minimization algorithms to use equilibrium constants of reactions in multiphase equilibrium calculations. Chemical Geology, 2016, 437, 170-181.	3.3	15
76	Nanoscale constraints on porosity generation and fluid flow during serpentinization. Geology, 2016, 44, 103-106.	4.4	68
77	Thermal damping and retardation in karst conduits. Hydrology and Earth System Sciences, 2015, 19, 137-157.	4.9	27
78	Corrigendum to "Thermal damping and retardation in karst conduits" published in Hydrol. Earth Syst. Sci., 19, 137–157, 2015. Hydrology and Earth System Sciences, 2015, 19, 451-451.	4.9	0
79	High performance reactive transport simulations examining the effects of thermal, hydraulic, and chemical (THC) gradients on fluid injectivity at carbonate CCUS reservoir scales. International Journal of Greenhouse Gas Control, 2015, 39, 285-301.	4.6	39
80	Brine displacement by CO2, energy extraction rates, and lifespan of a CO2-limited CO2-Plume Geothermal (CPG) system with a horizontal production well. Geothermics, 2015, 55, 182-194.	3.4	78
81	Implications of the redissociation phenomenon for mineral-buffered fluids and aqueous species transport at elevated temperatures and pressures. Applied Geochemistry, 2015, 55, 119-127.	3.0	9
82	CO2 sequestration in feldspar-rich sandstone: Coupled evolution of fluid chemistry, mineral reaction rates, and hydrogeochemical properties. Geochimica Et Cosmochimica Acta, 2015, 160, 132-154.	3.9	87
83	A comparison of electric power output of CO2 Plume Geothermal (CPG) and brine geothermal systems for varying reservoir conditions. Applied Energy, 2015, 140, 365-377.	10.1	115
84	CO2-Plume Geothermal (CPG) Heat Extraction in Multi-layered Geologic Reservoirs. Energy Procedia, 2014, 63, 7631-7643.	1.8	26
85	Internal consistency in aqueous geochemical data revisited: Applications to the aluminum system. Geochimica Et Cosmochimica Acta, 2014, 133, 216-234.	3.9	33
86	Experimental dissolution of dolomite by CO2-charged brine at 100°C and 150bar: Evolution of porosity, permeability, and reactive surface area. Chemical Geology, 2014, 380, 145-160.	3.3	94
87	Experimental Observation of Permeability Changes In Dolomite at CO ₂ Sequestration Conditions. Environmental Science & amp; Technology, 2014, 48, 140203132426009.	10.0	21
88	On the importance of the thermosiphon effect in CPG (CO2 plume geothermal) power systems. Energy, 2014, 69, 409-418.	8.8	97
89	Integrating CO2 Storage with Geothermal Resources for Dispatchable Renewable Electricity. Energy Procedia, 2014, 63, 7619-7630.	1.8	20
90	Numerical study of the effects of permeability heterogeneity on density-driven convective mixing during CO2 dissolution storage. International Journal of Greenhouse Gas Control, 2013, 19, 160-173.	4.6	32

#	Article	IF	CITATIONS
91	Geothermal Energy Production at Geologic CO2 Sequestration sites: Impact of Thermal Drawdown on Reservoir Pressure. Energy Procedia, 2013, 37, 6625-6635.	1.8	24
92	Permeability Reduction Produced by Grain Reorganization and Accumulation of Exsolved CO ₂ during Geologic Carbon Sequestration: A New CO ₂ Trapping Mechanism. Environmental Science & Technology, 2013, 47, 242-251.	10.0	32
93	DBCreate: A SUPCRT92-based program for producing EQ3/6, TOUGHREACT, and GWB thermodynamic databases at user-defined T and P. Computers and Geosciences, 2013, 51, 415-417.	4.2	53
94	Effects of permeability fields on fluid, heat, and oxygen isotope transport in extensional detachment systems. Geochemistry, Geophysics, Geosystems, 2013, 14, 1493-1522.	2.5	25
95	Developing Extensible Lattice-Boltzmann Simulators for General-Purpose Graphics-Processing Units. Communications in Computational Physics, 2013, 13, 867-879.	1.7	7
96	Process length scales and longitudinal damping in karst conduits. Journal of Geophysical Research, 2012, 117, .	3.3	30
97	Improved Characterization of Small " <i>u</i> ―for Jacob Pumping Test Analysis Methods. Ground Water, 2012, 50, 256-265.	1.3	6
98	Quantifying the effects of glacier conduit geometry and recharge on proglacial hydrograph form. Journal of Hydrology, 2012, 414-415, 59-71.	5.4	22
99	Mechanisms of heat exchange between water and rock in karst conduits. Water Resources Research, 2011, 47, .	4.2	47
100	Combining geothermal energy capture with geologic carbon dioxide sequestration. Geophysical Research Letters, 2011, 38, n/a-n/a.	4.0	166
101	Review: Geothermal heat as a tracer of large-scale groundwater flow and as a means to determine permeability fields. Hydrogeology Journal, 2011, 19, 31-52.	2.1	172
102	Performance analysis of singleâ€phase, multiphase, and multicomponent latticeâ€Boltzmann fluid flow simulations on GPU clusters. Concurrency Computation Practice and Experience, 2011, 23, 332-350.	2.2	36
103	Coupling carbon dioxide sequestration with geothermal energy capture in naturally permeable, porous geologic formations: Implications for CO2 sequestration. Energy Procedia, 2011, 4, 2206-2213.	1.8	139
104	Statistically reconstructing continuous isotropic and anisotropic two-phase media while preserving macroscopic material properties. Physical Review E, 2011, 83, 026706.	2.1	25
105	Interpolated lattice Boltzmann boundary conditions for surface reaction kinetics. Physical Review E, 2010, 82, 066703.	2.1	43
106	Three thousand years of extreme rainfall events recorded in stalagmites from Spring Valley Caverns, Minnesota. Earth and Planetary Science Letters, 2010, 300, 46-54.	4.4	38
107	Macroscale latticeâ€Boltzmann methods for low Peclet number solute and heat transport in heterogeneous porous media. Water Resources Research, 2010, 46, .	4.2	30
108	Accelerating Lattice Boltzmann Fluid Flow Simulations Using Graphics Processors. , 2009, , .		103

#	Article	IF	CITATIONS
109	A new partial-bounceback lattice-Boltzmann method for fluid flow through heterogeneous media. Computers and Geosciences, 2009, 35, 1186-1193.	4.2	92
110	Accelerating geoscience and engineering system simulations on graphics hardware. Computers and Geosciences, 2009, 35, 2353-2364.	4.2	58
111	A dimensionless number describing the effects of recharge and geometry on discharge from simple karstic aquifers. Water Resources Research, 2009, 45, .	4.2	51
112	Magma yield stress and permeability: Insights from multiphase percolation theory. Journal of Volcanology and Geothermal Research, 2008, 177, 1011-1019.	2.1	37
113	Numerical models of stiffness and yield stress growth in crystal-melt suspensions. Earth and Planetary Science Letters, 2008, 267, 32-44.	4.4	30
114	Lattice-Boltzmann Simulations of Carbonate Systems. , 2008, , .		1
115	Using pyrosequencing to shed light on deep mine microbial ecology. BMC Genomics, 2006, 7, 57.	2.8	405
116	Seasonal seismicity at western United States volcanic centers. Earth and Planetary Science Letters, 2005, 240, 307-321.	4.4	68
117	Quantifying magmatic, crustal, and atmospheric helium contributions to volcanic aquifers using all stable noble gases: Implications for magmatism and groundwater flow. Geochemistry, Geophysics, Geosystems, 2005, 6, n/a-n/a.	2.5	43
118	Depth dependence of permeability in the Oregon Cascades inferred from hydrogeologic, thermal, seismic, and magmatic modeling constraints. Journal of Geophysical Research, 2004, 109, .	3.3	161
119	Did melting glaciers cause volcanic eruptions in eastern California? Probing the mechanics of dike formation. Journal of Geophysical Research, 2004, 109, n/a-n/a.	3.3	103
120	Seismicity induced by seasonal groundwater recharge at Mt. Hood, Oregon. Earth and Planetary Science Letters, 2003, 214, 605-618.	4.4	168
121	Continuum percolation for randomly oriented soft-core prisms. Physical Review E, 2002, 65, 056131.	2.1	67
122	Numerical models of the onset of yield strength in crystal–melt suspensions. Earth and Planetary Science Letters, 2001, 187, 367-379.	4.4	177
123	Permeability-porosity relationship in vesicular basalts. Geophysical Research Letters, 1999, 26, 111-114.	4.0	266